Contemporary Mathematics
https://ojs.wiserpub.com/index.php/CM/

Research Article

Rational Bicubic Formulation of Dupin Cyclide

Iqra Saeed[1], Maria Hussain[1], Muhammad Farman[2,3,4*], Mohamad Hafeez[5,6], Faiza Sarfraz[7]

[1] Lahore College for Women University, Lahore, Pakistan
[2] Department of Mathematics, Faculty of Arts and Sciences, Near East University, Nicosia/Mersin 10, 99138, Turkey
[3] Faculty of Engineering and Natural Sciences, Istanbul Okan University, Istanbul, Turkey
[4] Research Center of Applied Mathematics, Khazar University, Baku, AZ1096, Azerbaijan
[5] Faculty of Engineering and Quantity Surveying, INTI International University Colleges, Nilai, Malaysia
[6] Faculty of Management, Shinawatra University, Pathum Thani, 12000, Thailand
[7] Faculty of Computer Science, Riphah International University, Gujranwala, Pakistan
E-mail: farmanlink@gmail.com

Received: 28 October 2025; **Revised:** 6 February 2026; **Accepted:** 6 February 2026

Abstract: Dupin cyclides are canal surfaces with circular lines of curvature and are widely used in geometric modelling applications such as Computer-Aided Design (CAD), surface fitting, and blending. In this research paper, we present a numerical approximation scheme for Dupin cyclide patches using rational bicubic Bézier surfaces. The boundary and interior control points are determined by enforcing C^1 continuity conditions, while the associated weights are optimized through curvature based variational fairness criterion. The complete Dupin cyclide is constructed by applying the suitable isometries to the constructed patches. The proposed approximation scheme interpolates the given cyclide data and ensures continuity across patch interfaces. The approximation quality is assessed using standard geometric error measures, including root mean square error and maximum relative error. Numerical experiments demonstrate that the maximum relative error attains the values of 0.6306 and 0.3982 for the two primary patches, confirming the computational efficiency of the proposed scheme.

***Keywords*:** Dupin cyclide, rational bicubic Bézier surface, surface fairing, variational fairness criteria, isometry

MSC: 65Y04, 51L20

1. Introduction

Cyclides are low-degree algebraic surfaces that are closed under offset, and their curvature lines are orthogonal circles [1]. Cyclides play a crucial role in the geometric modelling of free-form surfaces, architectural geometry, boundary representation in solid modelling, and surface blending (see references [1–3]). The cyclide surface serves as a fundamental component of both infrastructure development and industrial innovation. Through an analysis of cutting-edge designs and methods [4, 5], recent developments contribute to the future of industry. Bo et al. [3] presented a numerical optimization technique to fit free-form shapes with a cyclide spline. Suitable values of corner points and orthogonal frames at these corner points were estimated by minimizing the distance between interpolating cyclide surfaces and the target surfaces. Hoxhaj et al. [6] characterized all Dupin cyclides passing through a section of bicircular quartic planar curve. All Dupin

DOI: https://doi.org/10.37256/cm.7220269013

cyclides, admitting a given section, are classified as a surface of families that uniquely embeds into a Dupin cyclidic system. Garnier et al. [7] used Dupin cyclide for blending two quadrics of revolution. The authors used these blending techniques for geometric modelling of sea-horse and satellite antennas. Garnier et al. [8, 9] developed the algorithm to subdivide Dupin cyclide (ring, horned, and spindle) using quadratic Bézier curves with mass points. Alcázar, Dahlb and Muntingh [10] characterized the symmetric canal surfaces using a rational spine curve and radius function. The symmetric blends between two canal surfaces were also discussed. Zube and Krasauskas [11] introduced Möbius invariant bilinear rational representation for parameterization of Dupin cyclide with quaternions weights. Many classical properties were represented by the quaternion formula. Garnier et al. [12] discussed the conversion of biquadratic rational Bézier surfaces into torus and double sphere (special cases of Dupin cyclide). Zhou and Straßer [13] derived a Non-Uniform Rational B-Splines (NURBS) representation of a cyclide. First, the cyclide was reparametrized to the domain $[-1, 1]$. Then the blossom representation and control points at infinity were used to keep the representation compact and uniform.

The problem of constructing smooth, aesthetically pleasing and geometrically well behaved surfaces is closely related to broader research in surface approximation, surface fitting and fairness optimization. Huang et al. [14] aimed at the approximation of Weingarten surfaces using curvature based optimization technique. Zhu et al. [15] introduced a novel reconstruction of surfaces technique using partial differential equations and Coons patches. Tsuchie [16] proposed a curvature variation based fairness measure for curves for improving geometric evaluation and curve design by demonstrating automobile applications. Zafar and Hussain [17] discussed a novel method of construction of fair curves by controlling the curve length and curvature variation using rational cubic Said Ball curve. The shape parameters are obtained after optimizing the curvature variation and stretch energy as objective functional.

Despite the extensive theoretical study of Dupin cyclide and the development of various reparameterization, there are limited methods that translate cyclide into low degree rational Bézier patches with controllable shape parameters. The novel approximation technique presented in this work, is based on rational Bézier surfaces. It assures G^1 continuity, that is, calculates data values and derivatives at end points. Moreover, it has 8 free parameters which can improve the error of approximation as well as the geometric approximation of the surface. The geometric approximation strategy is adopted to compute the suitable value of the shape parameters, which has not been explicitly addressed in the existing literature. The shape design parameters are obtained by minimizing a fairness function that penalizes curvature variation to produce smooth surface. A suitable set of isometries is then applied to the approximated patches to generate a complete Dupin cyclide. The rational bicubic Bézier surface model is adopted in this work because it provides a low degree representation with sufficient degree of freedom through control points and weights. NURBS is the state of the art method for representation of surfaces. The NURBS and quaternion based approaches [11, 13] do not address the patch-wise numerical approximation under interpolation and continuity constraints. In the approach [13], cyclides are re-parameterized by NURBS through blossom representation, which neither interpolates cyclide data nor provides information about the continuity of the resulting approximation. Furthermore, the numerical scheme presented in [13] cannot proceed without introducing additional knots. In contrast, the approximation scheme proposed in this paper not only interpolates the data but it guarantees continuity across the surface. In [11], the principal patches of Dupin cyclides were parameterized by a rational Bézier surface with quaternion weights. The proposed construction [11] was not affine invariant, but it was Möbius invariant. The representation produced an implicit equation, principal curvatures, and representation as canal surfaces. As compared to [11], the Dupin cyclide approximation scheme proposed in this research paper is affine invariant. The proposed scheme is direct and performs well for any specified number of data points. Moreover, introducing rational polynomial functions provides more degrees of freedom through the inclusion of the weights, thereby increasing its effectiveness in designing free-form surfaces.

The paper is organized as follows. Section 2 discusses preliminaries. In Section 3, the rational bicubic approximation of Dupin cyclide is elaborated. In Section 4, free parameters are optimized according to the selected fairness measure. Section 5 is dedicated to error analysis. Isometries are applied on the approximated patches to obtain designing a complete surface in Section 6. Concluding remarks are highlighted in Section 7.

2. Preliminaries

In this section, the terms to be used in the next sections are reviewed.

2.1 *Dupin cyclides*

Dupin cyclides are canal surfaces having focal conics as its directrix. These are the envelopes of the variable spheres on one of the pair of focal conics and touches the sphere whose center is on its other focal conic [18]. Cyclides are categorized corresponding to the nature of the focal conics. Cyclides consisting of an ellipse and a hyperbola as focal conics are named as elliptic cyclides (non-degenerate) and those having two parabolas as focal conics are termed as parabolic cyclides (degenerate form). In extreme cases, if the hyperbola degenerates to a line and ellipse to a circle then the cyclide is a torus. Parametric equations of Dupin cyclides (non-degenerate) are the following.

$$\begin{aligned}
&S(\theta, \varphi) = (X(\theta, \varphi), Y(\theta, \varphi), Z(\theta, \varphi)),\\
&X(\theta, \varphi) = \frac{g_1(\theta, \varphi)}{g_4(\theta, \varphi)}, Y(\theta, \varphi) = \frac{g_2(\theta, \varphi)}{g_4(\theta, \varphi)}, Z(\theta, \varphi) = \frac{g_3(\theta, \varphi)}{g_4(\theta, \varphi)}, \theta, \varphi \in [0, 2\pi],\\
&g_1(\theta, \varphi) = m(c - a\cos\theta\cos\varphi) + b^2\cos\theta, g_2(\theta, \varphi) = b\sin\theta(a - m\cos\varphi),\\
&g_3(\theta, \varphi) = b\sin\varphi(c\cos\theta - m), g_4(\theta, \varphi) = a - c\cos\theta\cos\varphi.
\end{aligned} \tag{1}$$

The constants a, b, c are defined by the focal conics. The constants a, b, c are related as $c^2 = a^2 - b^2$ because of the condition of focal conics i.e. one conic is passing through the foci of the other. m describes the position of the center of moving spheres to the radius of the sphere. Each category of cyclide is further subdivided into three types depending upon the parameters m, a and c. For ring cyclide $c < m \leq a$, for horned cyclide $0 < m \leq c$ and spindle cyclide is generated for $m > a$ (Figure 1).

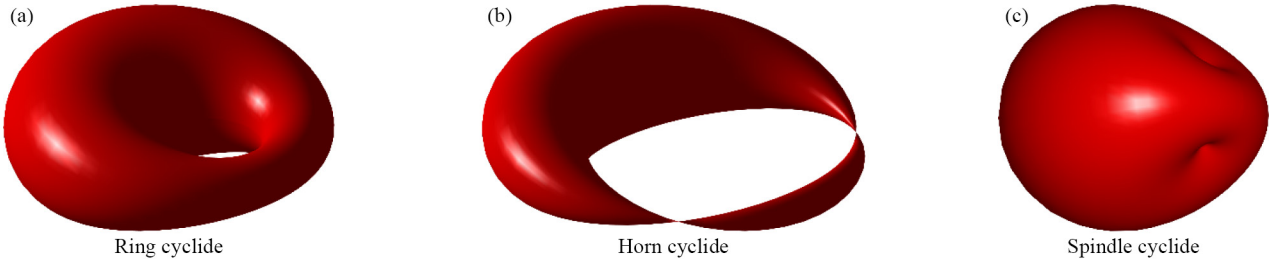

Figure 1. Three types of Dupin cyclides (non-degenerate form)

2.2 *Quasi-Newton method*

Quasi-Newton method [19] is a widely used algorithm for solving non-linear unconstrained optimization problems. It offers computational efficiency, particularly for the optimization problem involving large number of variables. In each iterative step, it updates the inverse of Hessian without solving it, making the quasi-Newton method less costly. For a problem of dimension n, the Quasi-Newton method converges in n-steps for the quadratic objective function. For the objective function of higher degree, the direction vector needs to be reinitialized in the direction of negative gradient generally after nth or $(n+1)th$ step. The process continues until the solution approaches the stopping criterion. As a gradient based technique, the Quasi-Newton method converges to a local minimum, not necessarily the global minimum.

3. Approximation of Dupin cyclide

This section introduces a numerical approximation framework for Dupin cyclide based on Rational Bicubic Bézier Surface (RBCBS) [12]. RBCBS is characterized by a set of control points, corresponding weights, and basic functions. The surface is defined as the following parametric expression:

$$P(u, v) = \frac{\sum_0^3 \sum_0^3 w_{ij} P_i(u) P_j(v) b_{ij}}{\sum_0^3 \sum_0^3 w_{ij} P_i(u) P_j(v)}, \; u, v \in [0, 1] \tag{2}$$

Here $(w_{ij})_{0\leq i,\, j\leq 3}$ represent weights and $(b_{ij})_{0\leq i,\, j\leq 3}$ are the control points. $P_i(u)$ and $P_j(v)$ are cubic Bernstein polynomials. Rational bicubic form depends upon the control points and the associated weights. Thus, it has a total of 32 degrees of freedoms (control points and weights). A good approximation scheme requires an adequate number of such degrees of freedom. In the proposed scheme, we calculate the control points by applying continuity constraints while the weights are treated as optimization variables to further refine the surface. Cyclides are geometrically complex figures (continuously varying tangents and curvatures). Therefore, it is not possible to approximate whole cyclide by single RBCBS. Approximation is carried out by dividing the whole surface into small patches. An arbitrary patch of Dupin cyclide is presented here as $S(\theta, \varphi)$, $(\theta, \varphi) \in [\theta_1, \theta_2] \times [\varphi_1, \varphi_2]$, $0 \leq \theta_1, \theta_2 \leq 2\pi$, $0 \leq \varphi_1, \varphi_2 \leq 2\pi$. The rational bicubic Bézier representation of Dupin cyclide patch is obtained by imposing the following conditions.

(i) The four corner points of cyclide patch and rational bicubic Bézier surface are used to calculate the corresponding corner control points of rational bicubic Bézier surface.

$$S(\theta_1, \varphi_1) = P(0, 0), \quad S(\theta_1, \varphi_2) = P(0, 1), \quad S(\theta_2, \varphi_1) = P(1, 0), \quad S(\theta_2, \varphi_2) = P(1, 1). \tag{3}$$

(ii) Similarly, the remaining boundary control points are computed by equating the following end point tangent interpolation condition.

$$S_\theta(\theta_1, \varphi_1) = P_u(u, v)|_{u=0,\, v=0}, S_\theta(\theta_1, \varphi_2) = P_u(u, v)|_{u=0,\, v=1} \tag{4}$$

$$S_\theta(\theta_2, \varphi_1) = P_u(u, v)|_{u=1,\, v=0}, S_\theta(\theta_2, \varphi_2) = P_u(u, v)|_{u=1,\, v=1} \tag{5}$$

$$S_\varphi(\theta_1, \varphi_1) = P_v(u, v)|_{u=0,\, v=0}, S_\varphi(\theta_1, \varphi_2) = P_v(u, v)|_{u=0,\, v=1} \tag{6}$$

$$S_\varphi(\theta_2, \varphi_1) = P_v(u, v)|_{u=1,\, v=0}, S_\varphi(\theta_2, \varphi_2) = P_v(u, v)|_{u=1,\, v=1} \tag{7}$$

Here S_θ and S_φ represent the tangent vectors along the parameters θ and φ at the corner points of Dupin cyclide patch. $P_u(u, v)$ and $P_v(u, v)$ are the tangent vectors of Rational Bicubic Bézier Surface (RBCBS) along u and v directions.

(iii) Central control points of the Bézier patch are evaluated by using twist vectors.

$$S_{\theta\varphi}(\theta_1, \varphi_1) = P_{uv}(u, v)|_{u=0,\, v=0}, S_{\theta\varphi}(\theta_1, \varphi_2) = P_{uv}(u, v)|_{u=0,\, v=1}, \tag{8}$$

$$S_{\theta\varphi}(\theta_2, \varphi_1) = P_{uv}(u, v)|_{u=1,\, v=0}, S_{\theta\varphi}(\theta_2, \varphi_2) = P_{uv}(u, v)|_{u=1,\, v=1}. \tag{9}$$

Using conditions (3)-(9), the following control points are calculated:

$$b_{00} = f_1,\, b_{30} = f_2,\, b_{03} = f_3,\, b_{33} = f_4,\, b_{10} = b_{00} + \frac{w_{00}}{3w_{10}} f_5,$$

$$b_{20} = b_{30} - \frac{w_{30}}{3w_{20}} f_6,\, b_{13} = b_{03} + \frac{w_{03}}{3w_{13}} f_7,\, b_{23} = b_{33} - \frac{w_{33}}{3w_{23}} f_8,\, b_{01} = b_{00} - \frac{w_{00}}{3w_{01}} f_9,$$

$$b_{02} = b_{03} - \frac{w_{03}}{3w_{02}} f_{11},\, b_{31} = b_{30} - \frac{w_{30}}{3w_{31}} f_{10},\, b_{32} = b_{33} - \frac{w_{33}}{3w_{32}} f_{12},$$

$$b_{11} = \frac{9b_{00}w_{00}w_{11} + 9w_{01}w_{10}\,(-2b_{00} + b_{01} + b_{10}) + w_{00}^2 f_{13}}{9w_{00}w_{11}},$$

$$b_{21} = \frac{9b_{30}w_{21}w_{30} + 9w_{20}w_{31}\,(b_{20} + 2b_{30} + b_{31}) - w_{30}^2 f_{14}}{9w_{30}w_{21}},$$

$$b_{12} = \frac{9b_{03}w_{12}w_{03} + 9w_{02}w_{13}\,(b_{02} - 2b_{03} + b_{13}) - w_{03}^2 f_{15}}{9w_{03}w_{12}},$$

$$b_{22} = \frac{9b_{33}w_{22}w_{33} + 9w_{23}w_{32}\,(b_{23} - 2b_{33} + b_{32}) + w_{33}^2 f_{16}}{9w_{33}w_{22}}, \tag{10}$$

where f_i's are given in appendix.

An arbitrary patch of the Dupin cyclide $[\theta_1,\ \theta_2] \times [\varphi_1,\ \varphi_2]$, where $0 \le \theta_1,\ \theta_2 \le 2\pi$, $0 \le \varphi_1,\ \varphi_2 \le 2\pi$ can be approximated using the calculated control points (10) of RBCBS. Substituting the x, y and z coordinates of the calculated control points $(b_{ij})_{0\le i,\, j\le 3}$ along with cubic Bernstein polynomials $P_i(u)$, $P_j(v)$ in equation (2), an RBCBS approximation of Dupin cyclide is obtained. A family of approximating surfaces is obtained by varying the weight parameters $(w_{ij})_{0\le i,\, j\le 3}$. These free parameters provide additional degrees of freedom for controlling the shape of the approximated surface. How to choose the best RBCBS approximation for given Dupin cyclide patch is an open question. In this research paper, the weights $(w_{ij})_{0\le i,\, j\le 3}$ are computed using the surface fairness criterion in the following section. Two patches are approximated using this representation over the parametric domain $\Omega_1 = \left[0,\, \frac{\pi}{2}\right] \times [0,\, \pi]$ and $\Omega_2 = \left[\frac{\pi}{2},\, \pi\right] \times [0,\, \pi]$.

4. Curvature minimization

Smoothness and fairness are central criteria in geometric modelling. Westgaard and Nowacki [20] provided detailed discussion of various second and higher order fairness measures. These measures based on different geometric properties of a surface, such as curvature or variation of curvature of the surface. In this study, Dupin cyclide is approximated using the curvature related fairness measure that depends upon the quadratic forms of partial derivatives of given surface $P(u,\, v)$. The resulting approximation is obtained by minimizing the fairness criterion $\chi(P) = \iint_\Omega (P_{uu}^2 + P_{vv}^2)\, du\, dv$. The optimization problem is stated as

$$\text{Minimize } \chi(P) = \text{Minimize } \iint_\Omega (P_{uu}^2 + P_{vv}^2)\, du\, dv \tag{11}$$

It can be seen from the above calculation that each boundary control point depends on two weight parameters, the weight associated with the boundary control point and the weight corresponding to the adjacent corner of the rectangular patch. Therefore, without loss of generality, the four weights associated with the corner control points are set to one. The optimization problem (11) will provide the appropriate values of free parameters $w'_{ij}s$ for fair patch. Here P^2_{uu} and P^2_{vv} are the second order partial derivatives of RBCBS with the control points $(b_{ij})_{1\leq i,\, j\leq 3}$ and the weights $(w_{ij})_{1\leq i,\, j\leq 3}$, calculated in Section 3. The integrals of P^2_{uu} and P^2_{vv} are evaluated by using Trapezoidal rule.

$$\int_0^1\int_0^1 P^2_{uu}\,du\,dv = \sum_{i=1}^{9}\|N_i\|^2, \qquad \int_0^1\int_0^1 P^2_{vv}\,du\,dv = \sum_{i=1}^{9}\|M_i\|^2 \tag{12}$$

Here $\|.\|$ is the Euclidean norm in $\mathbb{R}^3$. The computed values of M'_is and N'_is are provided in Appendix. The optimization problem (11) is solved in MATLAB using Quasi-Newton method discussed in Section 2. All the above discussion leads to the following algorithm.

Theorem 1 The Rational Bicubic Bézier Surface (RBCBS), defined in (1), approximate the Dupin cyclide if its control points are computed as

$$b_{00} = f_1,\, b_{30} = f_2,\, b_{03} = f_3,\, b_{33} = f_4,\, b_{10} = b_{00} + \frac{w_{00}}{3w_{10}}f_5,$$

$$b_{20} = b_{30} - \frac{w_{30}}{3w_{20}}f_6,\, b_{13} = b_{03} + \frac{w_{03}}{3w_{13}}f_7,\, b_{23} = b_{33} - \frac{w_{33}}{3w_{23}}f_8,$$

$$b_{01} = b_{00} - \frac{w_{00}}{3w_{01}}f_9,\, b_{02} = b_{03} - \frac{w_{03}}{3w_{02}}f_{11},\, b_{31} = b_{30} - \frac{w_{30}}{3w_{31}}f_{10},\, b_{32} = b_{33} - \frac{w_{33}}{3w_{32}}f_{12},$$

$$b_{11} = \frac{9b_{00}w_{00}w_{11} + 9w_{01}w_{10}\,(-2b_{00} + b_{01} + b_{10}) + w^2_{00}f_{13}}{9w_{00}w_{11}},$$

$$b_{21} = \frac{9b_{30}w_{21}w_{30} - 9w_{20}w_{31}\,(-b_{20} - 2b_{30} - b_{31}) - w^2_{30}f_{14}}{9w_{30}w_{21}},$$

$$b_{12} = \frac{9b_{03}w_{12}w_{03} + 9w_{02}w_{13}\,(b_{02} - 2b_{03} + b_{13}) - w^2_{03}f_{15}}{9w_{03}w_{12}},$$

$$b_{22} = \frac{9b_{33}w_{22}w_{33} + 9w_{23}w_{32}\,(b_{23} - 2b_{33} + b_{32}) + w^2_{33}f_{16}}{9w_{33}w_{22}}$$

and weights are computed by minimizing the surface fairness integral $\chi(P)$, defined in (11).

Algorithm 1. Details of the process shown in Figure 2 and steps are given below.

Step 1. First to approximate the Dupin cyclide by RBCBS over the rectangular patch $\Omega_1 = \left[0,\, \frac{\pi}{2}\right] \times [0,\, \pi]$. Input $\theta_1 = 0,\, \varphi_1 = 0,\, \theta_2 = \frac{\pi}{2},\, \varphi_2 = \pi$.

Step 2. Put values of $\theta_1,\, \varphi_1,\, \theta_2$ and φ_2 in $(b_{ij})_{0\leq i,\, j\leq 3}$ in set of equations (10), to calculate control points.

Step 3. Minimize $\chi(P)$ to obtain the fairest approximation of Dupin cyclide calculating most plausible values of weights.

Step 4. Substitute the values of control points and weights calculated in Step 2 and Step 3, to Theorem 1 to get the approximation of Dupin cyclide patch over the domain $\left[0, \frac{\pi}{2}\right] \times [0, \pi]$.

Step 5. Go to Step 1 to approximate Dupin cyclide over the domain $\Omega_2 = \left[\frac{\pi}{2}, \pi\right] \times [0, \pi]$.

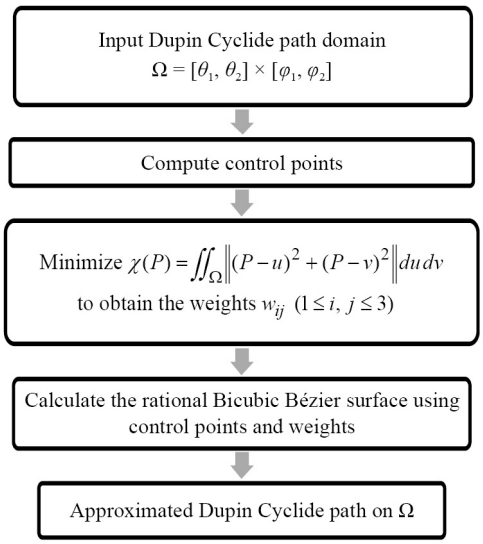

Figure 2. Algorithmic flowchart of proposed method

Algorithm 1 is applied to approximate the Dupin cyclide over two rectangular patches (see Figures 3-4). Table 1 shows the optimized values of the weights for each patch. The overall computational cost of the proposed approximation scheme is low and suitable for practical geometric modelling applications: as the evaluation of boundary and central control points involve only closed form algebraic expressions and only 12 weights are optimized using Quasi Newton method. As a result, the optimization converges quickly and each Dupin cyclide patch is generated within a fraction of a second in MATLAB. The efficiency of the proposed scheme is demonstrated by error analysis given in section 5.

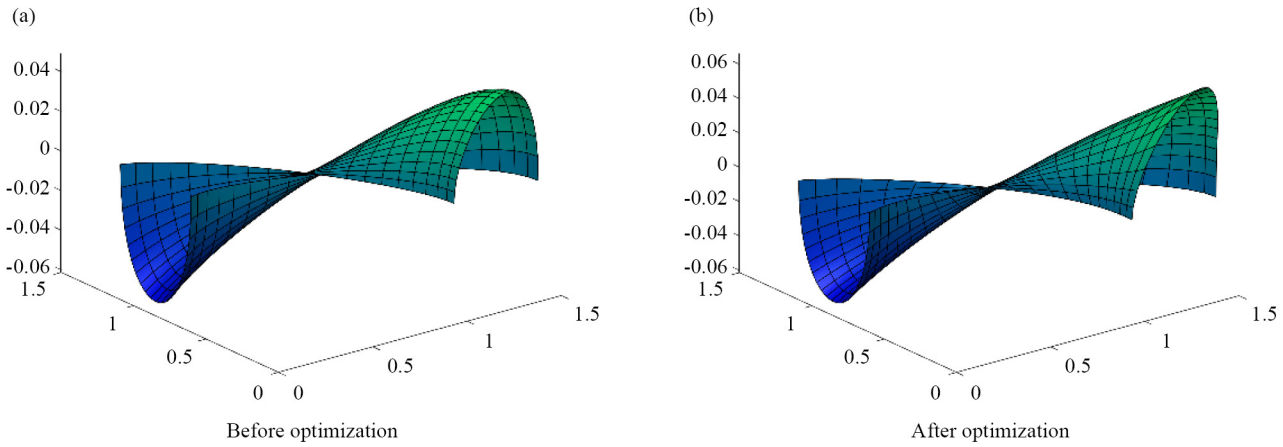

Figure 3. Dupin cyclide approximated patch Ω_1 for $a = 1$, $m = 0.25$, $c = 0.41$

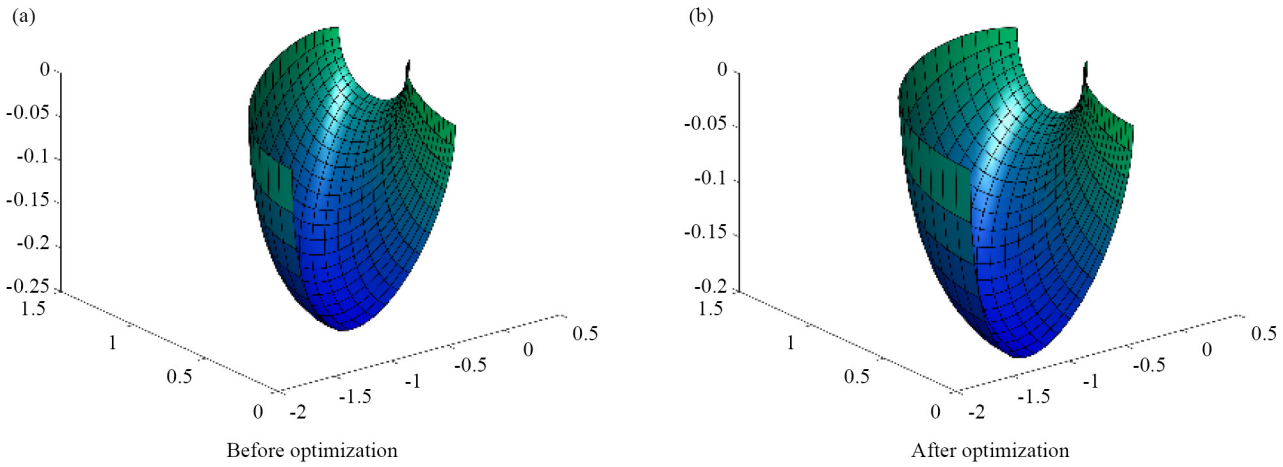

Figure 4. Dupin cyclide approximated patch Ω_2 for $a = 1$, $m = 0.25$, $c = 0.41$

Table 1. Values of weights

Weights	Optimized values of weights for Ω_1	Optimized values of weights for Ω_2
ω_{01}	1.6	1
ω_{10}	0.5480	0.7029
ω_{02}	-0.25	1
ω_{20}	1.2	0.8895
ω_{11}	0.765	0.765
ω_{12}	0.765	0.765
ω_{21}	0.755	0.8
ω_{23}	0.5	0.6025
ω_{13}	1.2	0.4607
ω_{22}	0.765	0.666
ω_{31}	0.9	1
ω_{32}	1.1	1.2

5. Error analysis

5.1 *Relative error*

The efficiency of the proposed numerical scheme can be analyzed by evaluating relative radius error for each patch. Error function is defined as $E = |e_1 - e_2|/|e_1|$ where $e_1 = x(\theta, \varphi)^2 + y(\theta, \varphi)^2 + z(\theta, \varphi)^2$ corresponds to the exact Dupin cyclide patch defined in (1) and $e_2 = \tilde{x}(u, v)^2 + \tilde{y}(u, v)^2 + \tilde{z}(u, v)^2$ is the radius function for the approximated patch. The reparameterization of θ, φ is considered corresponding to u, v for each patch to calculate the error. For the interval $[0, \frac{\pi}{2}] \times [0, \pi]$, the following reparameterization is used $\theta = u\frac{\pi}{2}$ and $\varphi = v\pi$ for $u, v \in [0, 1]$. The maximum relative error for the approximated patch Ω_1, is calculated to be 0.6306. Similarly, for the second patch defined over the interval $[\frac{\pi}{2}, \pi] \times [0, \pi]$, $\theta = (u+1)\frac{\pi}{2}$ and $\varphi = v\pi$ is used. The maximum relative error for second patch Ω_2, is found to be 0.2982.

5.2 *Root mean square error*

The Euclidean distance is defined as $D(u, v) = \|S(\theta, \varphi) - P(u, v)\|$ over $m \times n$ sample points for the given domain Ω. The root mean square error can be calculated as $RMSE = \sqrt{\frac{\sum_{(u,v)\in\Omega} D^2(u,v)}{r}}$, where $r = m \times n$ represents the total number of sample points.

Table 2 highlights the root mean square error and absolute maximum error of the proposed scheme for the two patches by taking 10×10 sampling points and using the reparameterization defined above. The table reports the magnitude of error before and after optimization of weights (whose optimal values are given in Table 1). The random values of weights before optimization are taken to be $\omega_{01} = -1$, $\omega_{10} = 1.5$, $\omega_{02} = 1$, $\omega_{20} = 1$, $\omega_{11} = 2$, $\omega_{13} = 1$, $\omega_{12} = -1$, $\omega_{21} = 1.5$, $\omega_{22} = 2$, $\omega_{23} = 1$, $\omega_{31} = 1.5$, $\omega_{32} = -1$. These metrics provide a measure of how closely rational bicubic Bézier surface approximates the Dupin cyclide across its domain. Figure 5 illustrates the RMSE surface map for the two patches Ω_1 and Ω_2.

Table 2. Error analysis

Errors	Error before optimizing weights	Error after optimizing weights
RMSE for Ω_1	1.6910	0.8274
RMSE for Ω_2	2.3763	1.8919
Relative error for Ω_1	1.1243	0.6306
Relative error for Ω_2	1.1041	0.2982

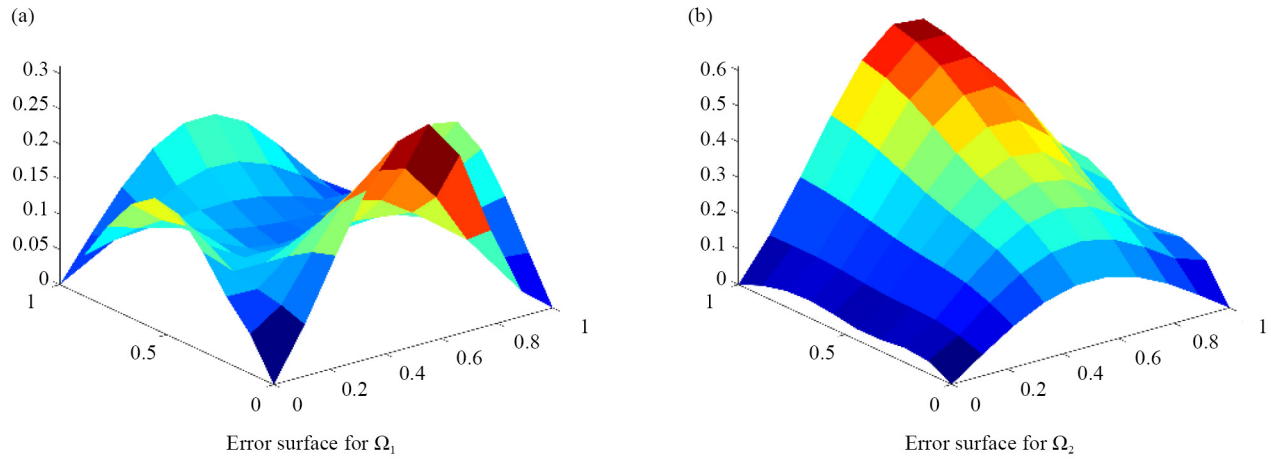

Figure 5. RMSE surface map for the two patches Ω_1 and Ω_2

The complete Dupin cyclide is approximated by applying the symmetry properties of Dupin cycle discussed in Section 6.

6. Construction of Dupin cyclide using isometries

An isometry g of R^3 is a mapping g: $R^3 \to R^3$ such that it leaves the surface S (or curve C) invariant [7]. Identity mapping is the trivial isometry. Non-trivial isometries include axial symmetries (rotation about axes), mirror symmetries (reflection about a plane), translations and their compositions [8]. A remarkable property of Dupin cyclide is that it

is symmetric about its planes containing focal conics. Here, to obtain complete Dupin surface, some of the nontrivial isometries are applied to two patches which are optimized by using the procedure defined in previous sections. Consider the first approximated cyclide patch, Ω_1, with optimized weights over the interval, $[\theta_1, \theta_2] \times [\varphi_1, \varphi_2]$, where $0 \leq \theta_1, \theta_2 \leq \frac{\pi}{2}$, $0 \leq \varphi_1, \varphi_2 \leq \pi$ (Figure 6(a)). As Ω_1 is symmetric about xy-plane so by applying the isometric transformation $g_1(x, y, -z)$ the mirror image is obtained as shown in Figure 6(b). Isometry $g_2(x, -y, z)$ generates third patch of Dupin cyclide (Figure 6(c)). Composition of these two isometries $g_3(x, -y, -z)$ or half-turn (rotation by angle π) about the line intersecting the planes of symmetry generates the fourth patch (Figure 6(d)).

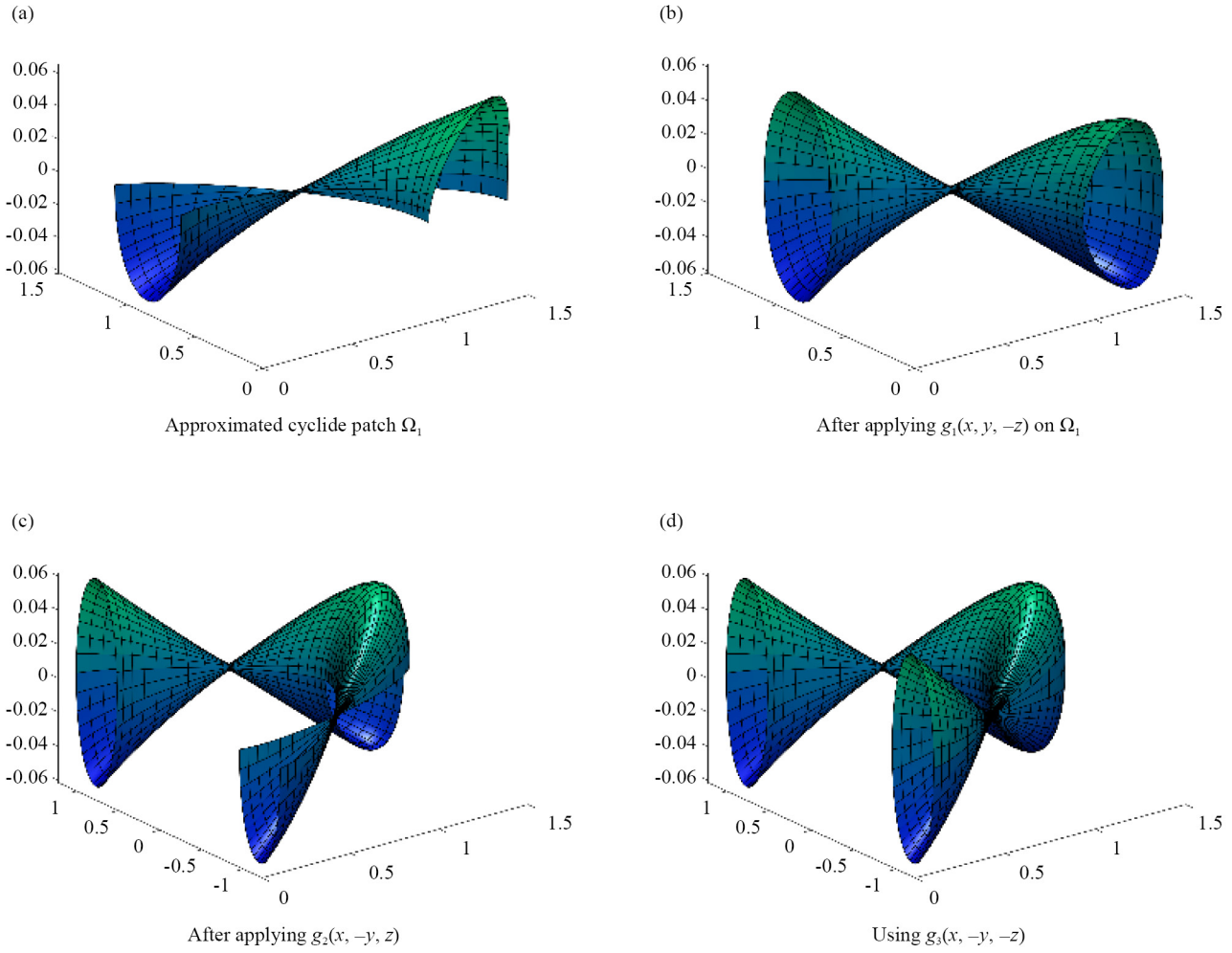

Figure 6. Approximated cyclide patch Ω_1 after applying isometries

Similarly, repeat the above-mentioned procedure for another cyclide patch, Ω_2, which is approximated by RBCBs in Section 4 for the interval $\left[\frac{\pi}{2}, \pi\right] \times [0, \pi]$. The set of isometries is again applied to obtain the remaining patches (symmetries of Ω_2) of Dupin cyclide as illustrated in Figure 7. Combination of two approximated patches Ω_1, Ω_2 and their symmetries approximate the complete Dupin cyclide surface (Figure 8).

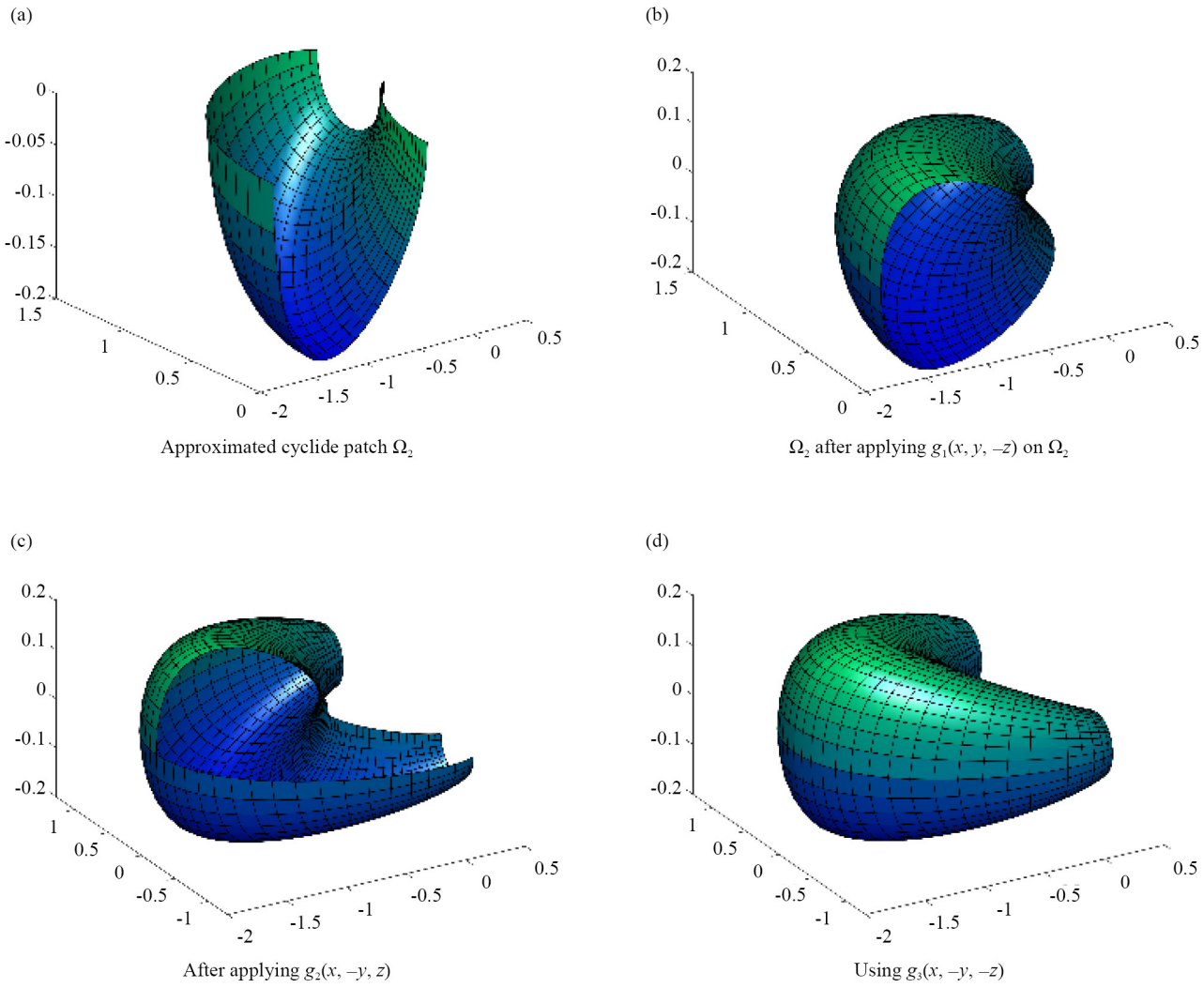

Figure 7. Approximated cyclide patch Ω_2 after applying isometries

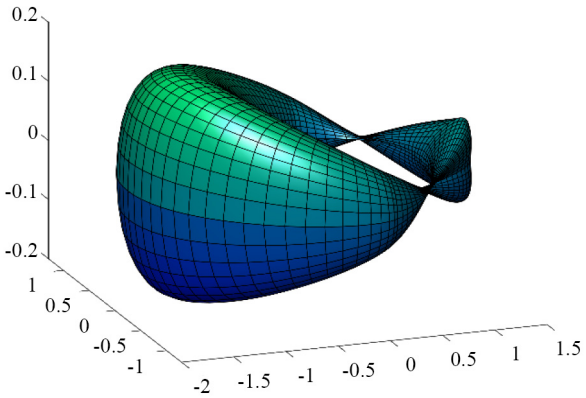

Figure 8. Complete Horn cyclide

7. Conclusion

This paper presents a rational bicubic Bézier surface approach to approximate Dupin cyclide patches defined over the domains $\left[0, \frac{\pi}{2}\right] \times [0, \pi]$ and $\left[\frac{\pi}{2}, \pi\right] \times [0, \pi]$. For each patch, the boundary and interior control points are calculated using C^1 continuity conditions. Optimization of the Bézier weights through a curvature based variational criterion provides additional flexibility and smoothness to each patch. Individual cyclide patches are constructed over the prescribed domain and suitable isometries are applied to obtain complete Dupin surface. Quantitative error analysis, including RMSE and absolute error metrics, confirmed the accuracy and robustness of the proposed approximation scheme.

The method provides a practical computational framework for applications in Computer-Aided Design (CAD), blending, architecture geometry and solid modelling, where smooth, low degree rational representation of cyclides are required [1–3]. However, the approach may have reduced flexibility for degenerate cyclide surfaces and the effectiveness of the fairness optimization depends on the choice of a suitable optimization strategy and appropriate initial values. Future work may extend the proposed framework to rational biquartic surface to increase modelling capacity and integrating adaptive patch refinement strategies for complex surface regions.

Conflict of interest

The authors declare no competing financial interest.

References

[1] Jia X. Role of moving planes and moving spheres following Dupin cyclides. *Computer Aided Geometric Design*. 2014; 31(3-4): 168-181.

[2] Menjanahary JM, Vidunas R. Dupin cyclides passing through a fixed circle. *Mathematics*. 2024; 12(10): 1505.

[3] Bo P, Liu Y, Tu C, Zhang C, Wang W. Surface fitting with cyclide splines. *Computer Aided Geometric Design*. 2016; 43: 2-15.

[4] Leong WY. *Industry 5.0: Design, Standards, Techniques and Applications for Manufacturing*. The Institution of Engineering and Technology; 2024.

[5] Juraev T, Abdukarimov T, Ubaydullayeva D, Fayziyev A, Xujakulov R. Simulation plow's body in solidworks by geometric data. In: *Epj Web of Conferences*. Vol. 321. EDP Sciences; 2025. p.01004.

[6] Hoxhaj E, Menjanahary JM, Krasauskas R. Sections of Dupin cyclides and their focal properties. *Journal of Symbolic Computation*. 2025; 129: 102402.

[7] Garnier L, Barki H, Foufou S. Dupin cyclide blends between non-natural quadrics of revolution and concrete shape modeling applications. *Computers Graphics*. 2014; 42: 31-41.

[8] Garnier L, Druoton L, Bécar JP, Fuchs L, Morin G. Subdivisions of ring Dupin cyclides using Bézier curves with mass points. *WSEAS Transactions on Mathematics*. 2021; 20: 581-596.

[9] Garnier L, Druoton L, Bécar JP, Fuchs L, Morin G. Subdivisions of horned or spindle Dupin cyclides using Bézier curves with mass points. *WSEAS Transactions on Mathematics*. 2021; 20: 756-776.

[10] Alcázara JG, Dahlb HEI, Muntingh G. Symmetries of canal surfaces and Dupin cyclides. *Computer Aided Design*. 2018; 59: 68-85.

[11] Zube S, Krasauskas R. Representation of Dupin cyclides using quaternions. *Graphical Models*. 2015; 82: 110-122.

[12] Garnier L, Belbis B, Foufou S. Conversion of biquadratic rational Bézier surfaces into patches of particular Dupin cyclides: the torus and the double sphere. In: *WSCG '2009: Communication Papers: Proceedings of the 17th International Conference in Central Europe on Computer Graphics, Visualization and Computer Vision in Co-Operation with Eurographics*. University of West Bohemia, Plzen. Czech Republic; 2009. p.101-108.

[13] Zhou X, Straßer W. A nurbs approach to cyclides. *Computers in Industry*. 1992; 19(2): 165-174.

[14] Huang F, Jiang C, Yang Y. Weingarten surface approximation by curvature diagram transformation. *Computer Aided Geometric Design*. 2025; 119: 102438.

[15] Zhu Z, Wang S, You L, Zhang J. Parametric surface reconstruction from 3D point data using partial differential equation and bilinearly blended coons patch. *Journal of Computation Physics*. 2024; 519: 113436.
[16] Tsuchie S. A new measure of fairness for curves. *Computer-Aided Design*. 2026; 190: 103979.
[17] Zafar S, Hussain M. Fair curve designing by Said-Ball curve. *PLoS One*. 2025; 20(7): 0324553.
[18] Farin G, Hoschek J, Kim MS. *Handbook of Computer Aided Geometric Design*. Elsevier Publisher; 2002.
[19] Rao SS. *Engineering Optimization Theory and Practice*. 4th ed. USA: John Wiley Sons; 2009.
[20] Westgaard G, Nowacki H. A process for surface fairing in irregular meshes. *Computer Aided Geometric Design*. 2001; 18(7): 619-638.

Appendix

The f_i's (for equation (10)) are given below:

$$f_1 = \left(\frac{g_1(\theta_1, \varphi_1)}{g_4(\theta_1, \varphi_1)}, \frac{g_2(\theta_1, \varphi_1)}{g_4(\theta_1, \varphi_1)}, \frac{g_3(\theta_1, \varphi_1)}{g_4(\theta_1, \varphi_1)}\right), f_2 = \left(\frac{g_1(\theta_2, \varphi_1)}{g_4(\theta_2, \varphi_1)}, \frac{g_2(\theta_2, \varphi_1)}{g_4(\theta_2, \varphi_1)}, \frac{g_3(\theta_2, \varphi_1)}{g_4(\theta_2, \varphi_1)}\right),$$

$$f_3 = \left(\frac{g_1(\theta_1, \varphi_2)}{g_4(\theta_1, \varphi_2)}, \frac{g_2(\theta_1, \varphi_2)}{g_4(\theta_1, \varphi_2)}, \frac{g_3(\theta_1, \varphi_2)}{g_4(\theta_1, \varphi_2)}\right), f_4 = \left(\frac{g_1(\theta_2, \varphi_2)}{g_4(\theta_2, \varphi_2)}, \frac{g_2(\theta_1, \varphi_2)}{g_4(\theta_2, \varphi_2)}, \frac{g_3(\theta_1, \varphi_2)}{g_4(\theta_2, \varphi_2)}\right),$$

$$f_5 = \left(\frac{g_5(\theta_1, \varphi_1)}{g_8(\theta_1, \varphi_1)}, \frac{g_6(\theta_1, \varphi_1)}{g_8(\theta_1, \varphi_1)}, \frac{g_7(\theta_1, \varphi_1)}{g_8(\theta_1, \varphi_1)}\right), f_6 = \left(\frac{g_5(\theta_2, \varphi_1)}{g_8(\theta_2, \varphi_1)}, \frac{g_6(\theta_2, \varphi_1)}{g_8(\theta_2, \varphi_1)}, \frac{g_7(\theta_2, \varphi_1)}{g_8(\theta_2, \varphi_1)}\right),$$

$$f_7 = \left(\frac{g_5(\theta_1, \varphi_2)}{g_8(\theta_1, \varphi_2)}, \frac{g_6(\theta_1, \varphi_2)}{g_8(\theta_1, \varphi_2)}, \frac{g_7(\theta_1, \varphi_2)}{g_8(\theta_1, \varphi_2)}\right), f_8 = \left(\frac{g_5(\theta_2, \varphi_2)}{g_8(\theta_2, \varphi_2)}, \frac{g_6(\theta_2, \varphi_2)}{g_8(\theta_2, \varphi_2)}, \frac{g_7(\theta_2, \varphi_2)}{g_8(\theta_2, \varphi_2)}\right),$$

$$f_9 = \left(\frac{g_9(\theta_1, \varphi_1)}{g_{12}(\theta_1, \varphi_1)}, \frac{g_{10}(\theta_1, \varphi_1)}{g_{12}(\theta_1, \varphi_1)}, \frac{g_{11}(\theta_1, \varphi_1)}{g_{12}(\theta_1, \varphi_1)}\right), f_{10} = \left(\frac{g_9(\theta_2, \varphi_1)}{g_{12}(\theta_2, \varphi_1)}, \frac{g_{10}(\theta_2, \varphi_1)}{g_{12}(\theta_2, \varphi_1)}, \frac{g_{11}(\theta_2, \varphi_1)}{g_{12}(\theta_2, \varphi_1)}\right),$$

$$f_{11} = \left(\frac{g_9(\theta_1, \varphi_2)}{g_{12}(\theta_1, \varphi_2)}, \frac{g_{10}(\theta_1, \varphi_2)}{g_{12}(\theta_1, \varphi_2)}, \frac{g_{11}(\theta_1, \varphi_2)}{g_{12}(\theta_1, \varphi_2)}\right), f_{12} = \left(\frac{g_9(\theta_2, \varphi_2)}{g_{12}(\theta_2, \varphi_2)}, \frac{g_{10}(\theta_2, \varphi_2)}{g_{12}(\theta_2, \varphi_2)}, \frac{g_{11}(\theta_2, \varphi_2)}{g_{12}(\theta_2, \varphi_2)}\right),$$

$$f_{13} = (g_{13}(\theta_1, \varphi_1), g_{14}(\theta_1, \varphi_1), g_{15}(\theta_1, \varphi_1)), f_{14} = (g_{13}(\theta_2, \varphi_1), g_{14}(\theta_2, \varphi_1), g_{15}(\theta_2, \varphi_1)),$$

$$f_{15} = (g_{13}(\theta_1, \varphi_2), g_{14}(\theta_1, \varphi_2), g_{15}(\theta_1, \varphi_2)), f_{16} = (g_{13}(\theta_2, \varphi_2), g_{14}(\theta_2, \varphi_2), g_{15}(\theta_2, \varphi_2)),$$

$$g_1(\theta_1, \varphi_1) = m(c - a\cos\cos\theta_1 \cos\varphi_1) + b^2 \cos\cos\theta_1,$$

$$g_2(\theta_1, \varphi_1) = b\sin\sin\theta_1 (a - m\cos\cos\varphi_1),$$

$$g_3(\theta_1, \varphi_1) = b\sin\sin\varphi_1 (c\cos\cos\theta_1 - m),$$

$$g_4(\theta_1, \varphi_1) = a - c\cos\cos\theta_1 \cos\varphi_1,$$

$$g_5(\theta_1, \varphi_1) = -\sin\theta_1 \left(ab^2 - ma^2\cos\varphi_1 + mc^2\cos\varphi_1\right),$$

$$g_6(\theta_1, \varphi_1) = -b(a - m\cos\cos\varphi_1),$$

$$g_7(\theta_1, \varphi_1) = -bc\sin\sin\varphi_1 \sin\theta_1 (a\varphi_1),$$

$$g_8(\theta_1, \varphi_1) = (a - c\cos\cos\theta_1 \cos\varphi_1)^2,$$

$$g_9(\theta_1, \varphi_1) = -c\cos\cos\theta_1 \sin\varphi_1 \left(mc^2 - ma^2 + b^2 c\cos\theta_1\right),$$

$$g_{10}(\theta_1, \varphi_1) = ab\sin\sin\varphi_1 \sin\theta_1 (m\theta_1),$$

$$g_{11}(\theta_1, \varphi_1) = -b(m - c\cos\cos\theta_1),$$

$$g_{12}(\theta_1, \varphi_1) = (a - c\cos\cos\theta_1\cos\varphi_1)^2,$$

$$g_{13}(\theta_1, \varphi_1) = \frac{\sin\sin\theta_1 \sin\varphi_1}{(a - c\cos\cos\theta_1\cos\varphi_1)^3}\left(-a^3 m + mac^2 - ma^2 c\cos\theta_1\cos\varphi_1\right.$$

$$\left. + mc^3\cos\theta_1\cos\varphi_1 + 2ab^2 c\cos\theta_1\right),$$

$$g_{14}(\theta_1, \varphi_1) = \frac{ab\sin\sin\varphi_1}{(a - c\cos\cos\theta_1\cos\varphi_1)^3}\left(-2cm\cos\varphi_1 + ma\cos\theta_1 + ca + cm\cos\varphi_1\cos^2\theta_1\right.$$

$$\left. + c^2\cos\varphi_1\cos\theta_1 - 2ac\cos^2\theta_1\right),$$

$$g_{15}(\theta_1, \varphi_1) = \frac{-bc\sin\sin\theta_1}{(a - c\cos\cos\theta_1\cos\varphi_1)^3}\left(am + a^2\cos\varphi_1 - 2am\cos^2\varphi_1 - 2ac\cos\theta_1\right.$$

$$\left. + ac\cos^2\varphi_1\cos\theta_1 + cm\cos\varphi_1\cos\theta_1\right).$$

The computed values of $M_i'S$ and $N_i'S$

$$M_1 = \frac{3}{2}\left(\frac{w_{02}}{w_{00}}(b_{02} - b_{00}) - 3\left(\frac{w_{01}}{w_{00}}\right)^2 (b_{01} - b_{00}) + \frac{w_{01}}{w_{00}}(b_{01} - b_{00})\right),$$

$$M_2 = \frac{3}{2}\left(\frac{w_{32}}{w_{30}}(b_{32} - b_{30}) - 3\left(\frac{w_{31}}{w_{30}}\right)^2 (b_{31} - b_{30}) + \frac{w_{31}}{w_{30}}(b_{31} - b_{30})\right),$$

$$M_3 = \frac{3}{2}\left(\frac{w_{01}}{w_{03}}(b_{01} - b_{03}) - 3\left(\frac{w_{02}}{w_{03}}\right)^2 (b_{02} - b_{03}) + \frac{w_{02}}{w_{03}}(b_{02} - b_{03})\right),$$

$$M_4 = \frac{3}{2}\left(\frac{w_{31}}{w_{33}}(b_{31} - b_{33}) - 3\left(\frac{w_{32}}{w_{33}}\right)^2 (b_{32} - b_{33}) + \frac{w_{32}}{w_{33}}(b_{32} - b_{33})\right),$$

$$M_5 = \frac{3}{\sqrt{2}r_1^3}\left(S_1^2 R_3 + \left(S_1^2 - 3S_1 S_2\right)R_2 + \left(3S_2^2 - S_1 S_3 - S_1 S_2\right)R_1\right),$$

$$M_6 = \frac{3}{\sqrt{2}r_4^3}\left(S_4^2R_2 + \left(S_4^2 - 18S_3S_4\right)R_3 + \left(18S_3^2 - 6S_4S_2 - 6S_3S_4R_4\right)\right),$$

$$M_7 = \sqrt{2}\left(K_1\left(w_{00} - 9w_{01} - 21w_{02} - 11w_{03}\right) + K_2\left(3w_{00} - 3w_{01} - 15w_{02} - 9w_{03}\right)\right.$$

$$+ K_3\left(5w_{00} + 3w_{01} - w_{02} - 7w_{03}\right) + K_4\left(7w_{00} + 9w_{01} - 3w_{02} - 5w_{03}\right)$$

$$\left. + K_5\left(9w_{00} + 15w_{01} + 3w_{02} - 3w_{03}\right) + K_6\left(11w_{00} + 21w_{01} + 9w_{02} - w_{03}\right)\right),$$

$$M_8 = \sqrt{2}\left(K_7\left(w_{30} - 9w_{31} - 21w_{32} - 11w_{33}\right) + K_8\left(3w_{30} - 3w_{31} - 15w_{32} - 9w_{33}\right)\right.$$

$$+ K_9\left(5w_{30} + 3w_{31} - w_{32} - 7w_{33}\right) + K_{10}\left(7w_{30} + 9w_{31} - 3w_{32} - 5w_{33}\right)$$

$$\left. + K_{11}\left(9w_{30} + 15w_{31} + 3w_{32} - 3w_{33}\right) + K_{12}\left(11w_{30} + 21w_{31} + 9w_{32} - w_{33}\right)\right),$$

$$M_9 = \sqrt{2}\left(K_{13}\left(S_1 - 9S_2 - 21S_3 - 11S_4\right) + K_{14}\left(3S_1 - 3S_2 - 15S_3 - 9S_4\right)\right.$$

$$+ K_{15}\left(5S_1 + 3S_2 - 9S_3 - 7S_4\right) + K_{16}\left(7S_1 + 9S_2 - 3S_3 - 5S_4\right)$$

$$\left. + K_{17}\left(9S_1 + 15S_2 + 3S_3 - 3S_4\right) + K_{18}\left(11S_1 + 21S_2 + 9S_3 - S_4\right)\right),$$

$$K_1 = 3w_{00}w_{01}\left(b_{01} - b_{00}\right),$$

$$K_2 = 3w_{00}w_{01}\left(b_{01} - b_{00}\right) + 6w_{00}w_{02}\left(b_{02} - b_{00}\right),$$

$$K_3 = 6w_{00}w_{02}\left(b_{02} - b_{00}\right) + 9w_{01}w_{02}\left(b_{02} - b_{01}\right) - 3w_{00}w_{03}b_{00},$$

$$K_4 = 3w_{00}w_{03}\left(b_{03} - b_{00}\right) + 9w_{01}w_{02}\left(b_{02} - b_{01}\right) + 6w_{01}w_{03}\left(b_{03} - b_{01}\right),$$

$$K_5 = 3w_{03}w_{02}\left(b_{03} - b_{02}\right) + 6w_{03}w_{01}\left(b_{03} - b_{01}\right),$$

$$K_6 = 3w_{02}w_{03}\left(b_{03} - b_{02}\right),$$

$$K_7 = 3w_{30}w_{31}\left(b_{31} - b_{30}\right),$$

$$K_8 = 3w_{30}w_{31}\left(b_{31} - b_{30}\right) + 6w_{30}w_{32}\left(b_{32} - b_{30}\right),$$

$$K_9 = 6w_{30}w_{32}\left(b_{32} - b_{30}\right) + 9w_{31}w_{32}\left(b_{32} - b_{31}\right) - 3w_{30}w_{33}b_{30},$$

$$K_{10} = 3w_{30}w_{33}(b_{33} - b_{30}) + 9w_{31}w_{32}(b_{32} - b_{31}) + 6w_{31}w_{33}(b_{33} - b_{31}),$$

$$K_{11} = 3w_{33}w_{32}(b_{33} - b_{32}) + 6w_{33}w_{31}(b_{33} - b_{31}),$$

$$K_{12} = 3w_{32}w_{33}(b_{33} - b_{32}),$$

$$K_{13} = 3(r_1R_2 - r_2R_1),$$

$$K_{14} = 6r_1R_3 + 3r_1R_2 - 3R_1(r_2 + 2r_1),$$

$$K_{15} = 3R_3(3r_2 + 2r_1) - R_2r_3 - 3R_1(r_4 + 2r_3),$$

$$K_{16} = 3R_4(2r_2 + r_1) + 9R_3r_2 - 3R_2(2r_4 + 3r_3) - 3R_1r_4,$$

$$K_{17} = 3R_4(r_3 + 2r_2) - 3R_3r_4 - 6R_2r_4,$$

$$K_{18} = 3R_4r_3 - 3R_3r_4,$$

$$R_1 = \frac{1}{8}(b_{00}w_{00} + 3b_{10}w_{10} + 3b_{20}w_{20} + b_{30}w_{30}),$$

$$R_2 = \frac{1}{8}(b_{01}w_{01} + 3b_{11}w_{11} + 3b_{21}w_{21} + b_{31}w_{31}),$$

$$R_3 = \frac{1}{8}(b_{02}w_{02} + 3b_{12}w_{12} + 3b_{22}w_{22} + b_{32}w_{32}),$$

$$R_4 = \frac{1}{8}(b_{03}w_{03} + 3b_{13}w_{13} + 3b_{23}w_{23} + b_{33}w_{33}),$$

$$S_1 = \frac{1}{8}(w_{00} + 3w_{10} + 3w_{20} + w_{30}),$$

$$S_2 = \frac{1}{8}(w_{01} + 3w_{11} + 3w_{21} + w_{31}),$$

$$S_3 = \frac{1}{8}(w_{02} + 3w_{12} + 3w_{22} + w_{32}),$$

$$S_4 = \frac{1}{8}(w_{03} + 3w_{13} + 3w_{23} + w_{33}),$$

$$N_1 = \frac{3}{2}\left(\frac{w_{20}}{w_{00}}(b_{20}-b_{00}) - 3\left(\frac{w_{10}}{w_{00}}\right)^2(b_{10}-b_{00}) + \frac{w_{10}}{w_{00}}(b_{10}-b_{00})\right),$$

$$N_2 = \frac{3}{2}\left(\frac{w_{23}}{w_{03}}(b_{23}-b_{03}) - 3\left(\frac{w_{13}}{w_{03}}\right)^2(b_{13}-b_{03}) + \frac{w_{13}}{w_{03}}(b_{13}-b_{03})\right),$$

$$N_3 = \frac{3}{2}\left(\frac{w_{10}}{w_{30}}(b_{10}-b_{30}) - 3\left(\frac{w_{20}}{w_{30}}\right)^2(b_{20}-b_{30}) + \frac{w_{20}}{w_{30}}(b_{20}-b_{30})\right),$$

$$N_4 = \frac{3}{2}\left(\frac{w_{13}}{w_{33}}(b_{13}-b_{33}) - 3\left(\frac{w_{23}}{w_{33}}\right)^2(b_{23}-b_{33}) + \frac{w_{23}}{w_{33}}(b_{23}-b_{33})\right),$$

$$N_5 = \frac{3}{\sqrt{2}s_1^3}\left(s_1^2 r_3 + \left(s_1^2 - 3s_1s_2\right)r_2 + \left(3s_2^2 - s_1s_3 - s_1s_2\right)r_1\right),$$

$$N_6 = \frac{3}{\sqrt{2}s_4^3}\left(s_4^2 r_2 + \left(s_4^2 - 3s_3s_4\right)r_3 + \left(3s_3^2 - s_4s_2 - s_3s_4\right)r_4\right),$$

$$\begin{aligned} N_7 = \sqrt{2}\,(&k_1(w_{00} - 9w_{10} - 21w_{20} - 11w_{30}) + k_2(3w_{00} - 3w_{10} - 15w_{20} - 9w_{30}) \\ &+ k_3(5w_{00} + 3w_{10} - w_{20} - 7w_{30}) + k_4(7w_{00} + 9w_{10} - 3w_{20} - 5w_{30}) \\ &+ k_5(9w_{00} + 15w_{10} + 3w_{20} - 3w_{30}) + k_6(11w_{00} + 21w_{10} + 9w_{20} - w_{30})), \end{aligned}$$

$$\begin{aligned} N_8 = \sqrt{2}\,(&k_7(w_{03} - 9w_{13} - 21w_{23} - 11w_{33}) + k_8(3w_{03} - 3w_{13} - 15w_{23} - 9w_{33}) \\ &+ k_9(5w_{03} + 3w_{13} - w_{23} - 7w_{33}) + k_{10}(7w_{03} + 9w_{13} - 3w_{23} - 5w_{33}) \\ &+ k_{11}(9w_{03} + 15w_{13} + 3w_{23} - 3w_{33}) + k_{12}(11w_{03} + 21w_{13} + 9w_{23} - w_{33})), \end{aligned}$$

$$\begin{aligned} N_9 = \sqrt{2}\,(&k_{13}(s_1 - 9s_2 - 21s_3 - 11s_4) + k_{14}(3s_1 - 3s_2 - 15s_3 - 9s_4) + k_{15}(5s_1 + 3s_2 \\ &- 9s_3 - 7s_4) + k_{16}(7s_1 + 9s_2 - 3s_3 - 5s_4) + k_{17}(9s_1 + 15s_2 + 3s_3 - 3s_4) \\ &+ k_{18}(11s_1 + 21s_2 + 9s_3 - s_4)), \end{aligned}$$

$$k_1 = 3w_{00}w_{10}(b_{10} - b_{00}),$$

$$k_2 = 3w_{00}w_{10}(b_{10} - b_{00}) + 6w_{00}w_{20}(b_{20} - b_{00}),$$

$$k_3 = 6w_{00}w_{20}(b_{20}-b_{00}) + 9w_{10}w_{20}(b_{20}-b_{10}) - 3w_{00}w_{30}b_{00},$$

$$k_4 = 3w_{00}w_{30}(b_{30}-b_{00}) + 9w_{10}w_{20}(b_{20}-b_{01}) + 6w_{10}w_{30}(b_{30}-b_{10}),$$

$$k_5 = 3w_{30}w_{20}(b_{30}-b_{20}) + 6w_{30}w_{10}(b_{30}-b_{10}),$$

$$k_6 = 3w_{20}w_{30}(b_{30}-b_{20}),$$

$$k_7 = 3w_{03}w_{13}(b_{13}-b_{03}),$$

$$k_8 = 3w_{03}w_{13}(b_{13}-b_{03}) + 6w_{03}w_{23}(b_{23}-b_{03}),$$

$$k_9 = 6w_{03}w_{23}(b_{23}-b_{03}) + 9w_{13}w_{23}(b_{23}-b_{13}) - 3w_{03}w_{33}b_{03},$$

$$k_{10} = 3w_{03}w_{33}(b_{33}-b_{03}) + 9w_{13}w_{23}(b_{23}-b_{13}) + 6w_{13}w_{33}(b_{33}-b_{13}),$$

$$k_{11} = 3w_{33}w_{23}(b_{33}-b_{23}) + 6w_{33}w_{13}(b_{33}-b_{13}),$$

$$k_{12} = 3w_{23}w_{33}(b_{33}-b_{23}),$$

$$k_{13} = 3r_1R_2 - 3r_2R_1,$$

$$k_{14} = 6R_3r_1 + 3R_2r_1 - 3R_1(r_2+2r_1),$$

$$k_{15} = 3R_3(3r_2+2r_1) - 9R_2r_3 - 3R_1(r_4+2r_3),$$

$$k_{16} = 3R_4(2r_2+r_1) + 9R_3r_2 - 3R_2(2r_4+3r_3) - 3R_1r_4,$$

$$k_{17} = 3R_4(r_3+2r_2) - 3R_3r_4 - 6R_2r_4,$$

$$k_{18} = 3R_4r_3 - 3R_3r_4,$$

$$r_1 = \frac{1}{8}(b_{00}w_{00} + 3b_{01}w_{01} + 3b_{02}w_{02} + b_{03}w_{03}),$$

$$r_2 = \frac{1}{8}(b_{10}w_{01} + 3b_{11}w_{11} + 3b_{12}w_{12} + b_{13}w_{13}),$$

$$r_3 = \frac{1}{8}(b_{20}w_{20} + 3b_{21}w_{21} + 3b_{22}w_{22} + b_{23}w_{23}),$$

$$r_4 = \frac{1}{8}\left(b_{30}w_{30} + 3b_{31}w_{31} + 3b_{32}w_{32} + b_{33}w_{33}\right),$$

$$s_1 = \frac{1}{8}\left(w_{00} + 3w_{01} + 3w_{02} + w_{02}\right),$$

$$s_2 = \frac{1}{8}\left(w_{10} + 3w_{11} + 3w_{12} + w_{13}\right),$$

$$s_3 = \frac{1}{8}\left(w_{20} + 3w_{21} + 3w_{22} + w_{23}\right),$$

$$s_4 = \frac{1}{8}\left(w_{30} + 3w_{31} + 3w_{33} + w_{33}\right).$$